

Effect of pressure dependence on N.E.C of Argon thermal plasmas mixed with Helium

F. Boudahri^a, A. K. Ferouani^{b,c}, B. Liani^c, S. Ailas^c and M. Lemerini^c

^a*Faculty of Science and Technology,
University of Relizane, 48000, Algeria.*

^b*Ecole Supérieure en Sciences Appliquées, Tlemcen, 13000, Algeria.*

^c*L.P.T Laboratory, University A. Belkaid of Tlemcen, 13000, Algeria.
e-mail: ferouani_karim@yahoo.fr*

Received 1 January 2022; accepted 9 February 2022

In the present work, we have calculated the radiative transfer, it means the radiative energy that escapes from a plasma formed from a mixture of Argon–Helium. The computations take into account several pressures between $1 \leq p \leq 100$ atm in the temperature T wide range of 5000 – 30 000 K. In the case of the plasmas is supposed to be in local thermodynamic equilibrium. Where the contributions have been treated separately in the calculation: atomic emission lines self-absorbed and not self-absorbed, continuum (radiative attachment, radiative recombination and radius). The results show that a large part of radiation is absorbed at the first crossed millimeter and also the contribution of resonance lines is very important. These are the lines which are strongly absorbed.

Keywords: Plasma simulation; Plasma diagnostic; Net emission; Radiation; Argon–Helium.

DOI: <https://doi.org/10.31349/RevMexFis.68.041501>

1. Introduction

Argon plasmas have a wide range of applications in both research and industry. Metal vapour, particularly iron vapour, can penetrate the Argon plasma and alter its properties in a number of these applications. Tungsten inert gas welding, metal inert gas welding, plasma spraying of metallic particles, metal ladle heating, scrap metal heating, and tundish heating are only a few examples of applications [1–4].

Thermal plasmas created by plasma torches and electrical arcs are being used in a growing number of industrial applications. This method has numerous applications in metallurgy, the steel industry, and the large field of materials research. The development of these techniques and their improvement require time consuming and expensive practical tests. Thermal plasma radiative transfer is studied in order to develop physical and/or numerical models of these approaches, which are characterized by high temperature energy exchanges. Radiation is therefore an essential term in the energy balance which has to be taken into account in any model [5].

N.E.C (Net Emission Coefficient) is useful in determining the amount of radiant energy lost from a plasma. In a number of plasma analyses (see *e.g.*, [6–8]). N.E.C are basic representations of the radiative source term, however given the options of completing a full radiative source term analysis [9] or using the method of partial characteristics [10] N.E.C are useful. Some comparisons of results determined by using N.E.C and other methods are given by J. J. Lowke (1974) [11].

An estimated approach of accounting for radiative transmission of energy in thermal plasmas is computationally convenient of N.E.C of radiation. Because the energy balance equation at the arc center is driven by a balance between ra-

diation losses and ohmic heating, these coefficients significantly dictate computed values of central arc temperatures. Even though the method cannot predict the absorption in the plasma regions with steep temperature gradients, it is widely used in computational flow dynamics (see *e.g.* S. Ailas *et al.* [6] and S. Ailas [12]).

A. Gleizes *et al.* 1993 [8] calculate the net emission coefficient using the line escape factor approach (H. W. Drawin and F. Emard 1973 [13]) for the stronger lines, while assuming the weaker lines to be optically thin. Both of these assumptions are good for many conditions, but certain situations exist where inaccuracies can result. A large number of lines are used for all atomic and ionic species. Our study deals with the calculation of the N.E.C for isothermal and homogeneous plasmas, for instance, in the articles by [14–17].

To eliminate, B. Liani *et al.* (1997) [18] have studied the evaluation of the N.E.C in total radiation which escapes from a plasma mixture of CH₄-H₂. Only in this research [18], the contribution of the diatomic molecular bands was neglected so that the results are valid for temperature $T \geq 5000$ K.

The N.E.C is then calculated in a classical way for thermal plasmas, *i.e.* considering an isothermal plasma sphere of radius R_p . The results are presented for atmospheric thermal plasmas in a temperature range between 5000 and 30 000 K, and various gas proportions in the mixture.

The first part of this work is devoted to a brief description of the considered chemical species and to the method used to obtain the equilibrium composition of the plasma. The second part presents the calculation of the radiative properties with the N.E.C method, has been devoted to calculate the radiative properties of the plasma including the determination of absorption coefficients of the N.E.C which represents the total power radiated by the plasma. The contributions have

been treated separately in the calculation: atomic emission self-absorbed lines and not self-absorbed lines, continuum (radiative attachment, radiative recombination and radius).

2. Plasma composition

The first step consists in calculating the equilibrium composition of the plasma versus the temperature and the pressure, only the following gaseous species are taken into account: electrons, Ar, He, Ar⁺, He⁺, Ar²⁺, He²⁺ and Ar³⁺.

The numerical method used to calculate the equilibrium composition of the plasma is based upon the mass action law and on the basic chemical concept defined by S. Askri *et al.* [19]. This law enables the generation of as many equations as there are independent chemical processes existing in a plasma. This law is written as follows for a specific reaction [20]:

$$\prod_{i=1}^N n_i^{v_i} = \prod_{i=1}^N (Q_{\text{Tot,Vol}}^i)^{v_i} \quad (1)$$

with N the total number of chemical species considered in this reaction, v_i the corresponding stoichiometric coefficients, n_i and $Q_{\text{Tot,Vol}}^i$ the species population density i and total volumetric partition function, respectively. $Q_{\text{Tot,Vol}}^i$ is given by:

$$Q_{\text{Tot,Vol}}^i(T) = \left(\frac{2\pi m_i k_B T}{h^2} \right)^{3/2} \times Q_{\text{int}}^i(T) \exp\left(\frac{-E_i^{\text{ret}}}{k_B T} \right), \quad (2)$$

where $Q_{\text{int}}^i(T)$ is the internal partition function of the species i and E_i^{ret} its reference energy calculated from the formation enthalpy defined in JANAF tables [21]. The partition function must be understood to calculate plasma composition. This step requires a large amount of data which can be determined either from the literature or thanks to appropriate formulae depending on the nature of the species: atomic or molecular species [22]. Internal partition functions of atoms and their positive ions are taken from [13], internal partition functions were assumed to be equal to the degeneracy of the ground state for negative atomic ions, they were calculated with the Morse potential minimization method [22] for diatomic species. The spectroscopic data (Dunham coefficients, vibrational frequencies and degeneracies, rotational constants, moments of inertia and symmetry numbers) essential to the calculation of the internal partition functions of molecules were taken from M. W. Chase *et al.* [21] and K. P. Huber *et al.* [23].

Finally, the charged species create a Coulombian field, which modifies the plasma's state by creating an interaction potential. When the population number densities of charged particles are important at high temperatures, this impact is critical. The interactions between neutral particles also indicate a modification of the perfect gas law at low temperatures and pressures higher than atmospheric pressure. Therefore,

the Debye–Hückel and the Viriel corrections [24] have been considered.

3. Theoretical background for N.E.C in spherical symmetry

The calculation of the N.E.C is based upon simplifying assumptions concerning the plasma geometry, the plasma is supposed to be homogeneous, spherical and isothermal [25–27]. The local thermodynamic equilibrium hypothesis is also considered. Of course, in most cases, the geometry of a thermal plasma is cylindrical and not spherical but it has been demonstrated that the N.E.C at the centre of a sphere is close to the one obtained on the axis of an infinite cylinder [28]. The N.E.C is defined by the difference between the power radiated by a unit volume and the radiation proceeding from the other regions of the plasma and absorbed in this unit volume.

For a spherical geometry, the N.E.C (in W m⁻³ sr⁻¹) is written as follows (more details of the implementation in the N.E.C can be found in [29, 30]):

$$\varepsilon_N(T, R_p) = \int_0^\infty B_\lambda(T) k'_\lambda(T) \exp[-k'_\lambda(T) R_p] d\lambda, \quad (3)$$

where λ is the wavelength, B_ν is the Planck function [31], R_p is the plasma radius and k'_ν is the monochromatic absorption coefficient corrected for the effects of induced emission and correlated with the local emission coefficient ε_ν by the Kirchhoff law [31]:

$$\varepsilon_\lambda(T) = B_\lambda(T) \cdot k'_\lambda(T). \quad (4)$$

The monochromatic absorption coefficient:

$$k'_\lambda(T) = k_\lambda(T) \left(1 - \exp\left[-\frac{hc}{\lambda k_B T} \right] \right), \quad (5)$$

where h and k_B are the Planck and Boltzmann constants, c is the light velocity and k_ν is the total absorption coefficient.

3.1. Emission of the continuum

In thermal plasmas, the continuum radiation is produced by four radiative processes [6]. To calculate the variation of the molecular absorption coefficient with the temperature, it is assumed that the absorption cross section does not depend on temperature. As excited electronic molecular states become populated when the temperature increases, the continuum absorption coefficient is thus underestimated with this simplifying assumption. It is given by [12]:

$$K_\lambda^{\text{cont-mol}}(T) = N_{\text{mol}}(T) \cdot \sigma_{\text{abs}}(\lambda), \quad (6)$$

where N_{mol} being the number density of the molecule and σ_{abs} indicate photo-absorption cross section [12].

3.2. Net emission of lines

The N.E.C of the lines is calculated with the assumption there are two types of lines defined by their self-absorption coefficients. If the transition of the line involves a low level close to the fundamental, it will be considered to be self-absorbed, this term means that the radiation emitted by the atom is re-absorbed in the plasma (photo-excitation mechanism). The others lines will be assumed to be light, crossing the medium without being absorbed (as if it were optically thin) and having a close leakage factor of 1. To make this selection which saves considerable time in calculations, we referred to the energy levels given by the literature [18, 32].

3.2.1. Net emission of not self-absorbed lines

These lines are low-intensity and poorly absorbed in plasma. This helps to simplify Eq. (3) by removing the terms of self-absorption such as the leakage factor and/or exponential term. Thus the net emission coefficient of lines not self-absorbed is written as follows (more details see the references [7]):

$$\varepsilon_N^{\text{non-aut}} = \sum_{\lambda_0} B_{\lambda_0}^0(T) k_{\lambda_0}(T) \times \left(1 - \exp \left[-\frac{hc}{\lambda_0 k_B T} \right] \right). \quad (7)$$

3.2.2. Net emission of self-absorbed lines

For these lines, the net emission calculation takes into account the absorption effects in plasma through the leakage factor. In general, highly absorbed lines are the resonance lines (transitions leading to the fundamental level). The coefficient net emission of self absorbed lines is therefore obtained by the following relation (more details see the references [7]):

$$\varepsilon_N^{\text{aut}} = \sum_{\lambda_0} B_{\lambda_0}^0(T) k'_{\lambda_0}(T) \Lambda_r(\alpha, \tau_0) \times \exp \left(-k'_{c, \lambda_0}(T) R_p \right), \quad (8)$$

where $\Lambda_r(\alpha, \tau_0)$ is the leakage factor [13] which depends on the optical thickness τ_0 center of the line and its total enlargement through the coefficient α .

As mentioned that the total net emission factor is the sum of the three contributions: the net emission due to the atomic continuum, the emission of self-absorbed lines and not self-absorbed lines [32]:

$$\varepsilon(T, R_p) = \varepsilon_N^{\text{cont}}(T, R_p) + \varepsilon_N^{\text{aut}}(T, R_p) + \varepsilon_N^{\text{not-aut}}(T, R_p). \quad (9)$$

4. Results and discussions

It should be mentioned for calculating the partition functions of different species, we used values from the literature *reference energies*: JANAF tables [21], *Internal partition function of atomic species*: [33], *Internal partition function of*

diatomic species: JANAF data [21] and [22], *Continuum radiation*: NIST database [34] and [35], *Lines radiation*: NIST database [34] and [36–38].

4.1. Equilibrium composition

In Fig. 1, we plot the plasma composition obtained for equilibrium composition of a 50% Ar–50% He mixture as a function of the temperature in the range between 5000 and 30 000 K, shown for four selected pressure values: (a) $p = 1$ atm, (b) $p = 4$ atm, (c) $p = 10$ atm and (d) $p = 100$ atm. The first phase is characterized by dominance of the species Ar, He in a temperature range ranging from 5000–15 000 K, with the gradual appearance of species Ar^+ , He^+ and Ar^{2+} . Because of their low ionization potential, the species Ar^+ are more dominant by relation to the ion He^+ . When the temperature is between 15 000 – 30 000 K, we note that the elections are the dominant. On the other hand, in the Fig. 1c) (*i.e.* $p = 10$ atm, for example) we plotted the evolution of densities (higher pressure value), we note that species densities are significantly proportional to plasma pressure.

By examining these curves, we note the strong presence of Ar up to a temperature close to ~ 15 000 K, where it begins to decrease, indeed, the species Ar^+ and e^- become majority at a temperature close to ~ 15 000 K up to the temperature 30 000 K. It should also be noted that the ion Ar^+ ensures the electrical neutrality of the plasma with the electrons in the temperature range 15 000–30 000 K, the Ar^{2+} species begins to appear from ~ 12 000 K, the other by the Ar^{3+} species remains very low in the temperature range considered.

It is clear that the inclusion of the calculation of the composition of a plasma in thermodynamic equilibrium shows that the densities of the species present in the plasma are not independent, they are dependent on temperature and pressure. For the pressure, we can say that the densities of the species are appreciably proportional to the pressure of the plasma, and for the temperature, we see that the density of the atomic species will decrease (slightly) for large temperatures (due to ionization), however, the densities of the charged species will increase.

Figure 2 compares the number density obtained in the case of pure plasmas Ar and He and binary mixtures 50% Ar–50% He and 80% Ar–20% He at atmospheric pressure and $R_p=0$ mm. The ionization energies of Ar and He being close, a slight difference in the number density for these two pure plasmas or mixtures can be noticed in this temperature range. Between 25 000–30 000 K, the number density decreases by some $\sim 9\%$ for pure Ar or He plasmas while it decreases by approximately $\sim 17\%$ in the case of a plasma. On the other hand, for temperatures lower than 15 000, the number density for pure He plasmas is largely lower than the number densities for pure Ar. This result is due to the high ionization energy of the neutral He (24.58 eV) in contrast to the ionization energies of Ar (15.76 eV).

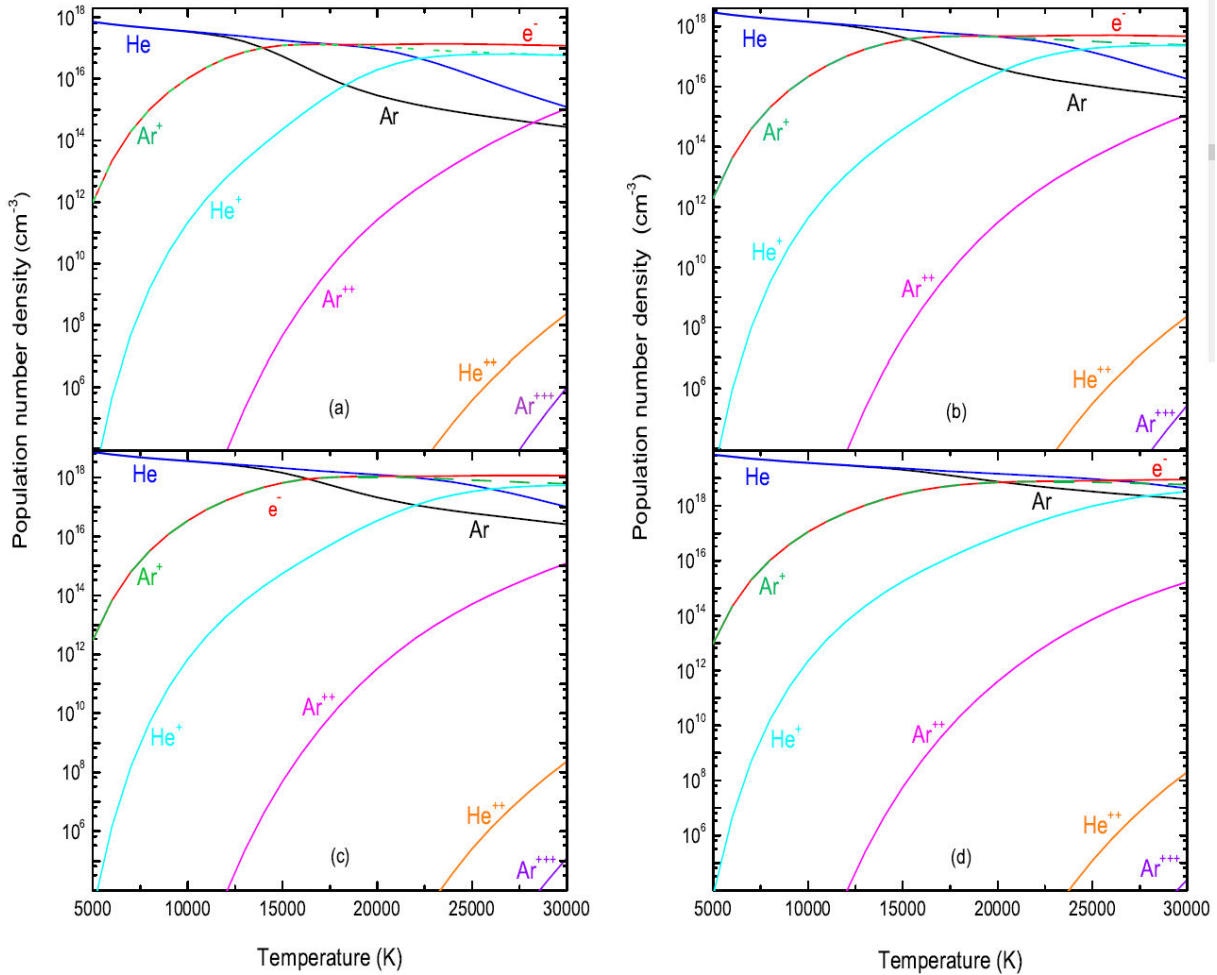


FIGURE 1. Equilibrium composition of 50% Ar–50% He mixture as a function of the temperature, shown for four selected pressure values: a) $p = 1$ atm, b) $p = 4$ atm, c) $p = 10$ atm and d) $p = 100$ atm.

4.2. N.E.C of continuum

The N.E.C of a plasma of radius R_p at atmospheric pressure and temperature T , is given by expression (3). We calculated the N.E.C of the continuum as a function of the temperature and the thickness of the plasma, the results obtained concerning the 50% Ar–50% He mixture, for plasma thickness $R_p = 0$ mm are shown in Fig. 3. The contribution to the influence of each of the 2 species is represented there. $R_p = 0$ mm corresponds to the fictitious case of an optically thin plasma, for which absorption is considered zero. We note that He does not take a large part in the total radiation of the continuum.

- It is, therefore, Argon species that mainly contributes to the radiation of the mixture 50% Ar–50% He.
- For temperatures $T \geq 19000$ K, Ar is the species that radiates the most. Indeed, the densities of the ions Ar^+ and Ar^{2+} are majority at these temperatures.

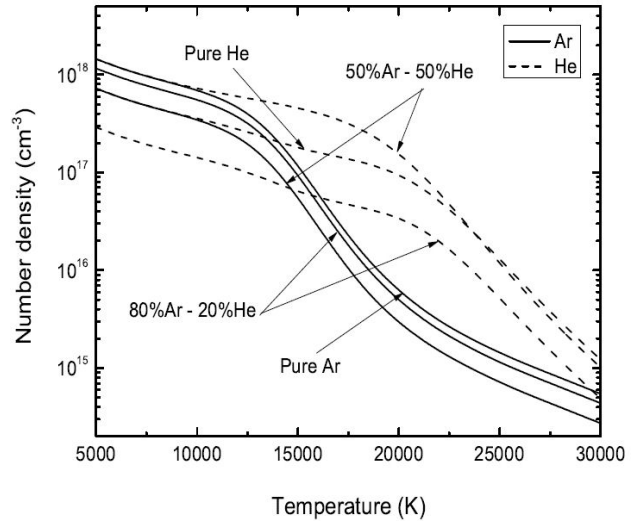


FIGURE 2. Number density for pure gases, 50% Ar–50% He and 80% Ar–20% He mixtures at atmospheric pressure.

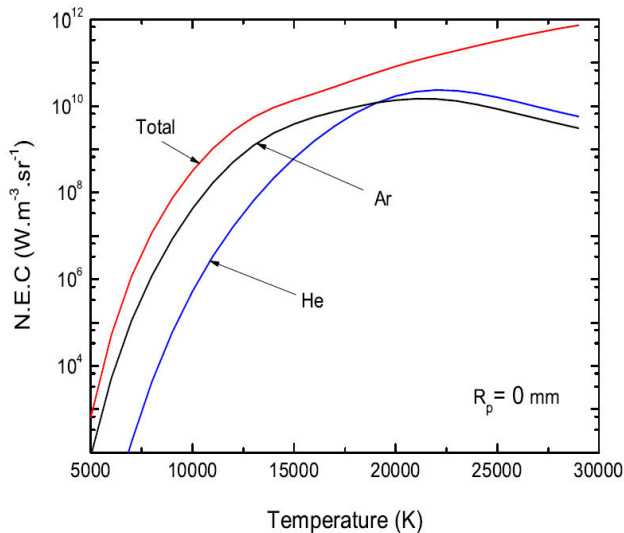


FIGURE 3. N.E.C of the continuum of an optically thin plasma of a mixture 50% Ar–50% He at atmospheric pressure.

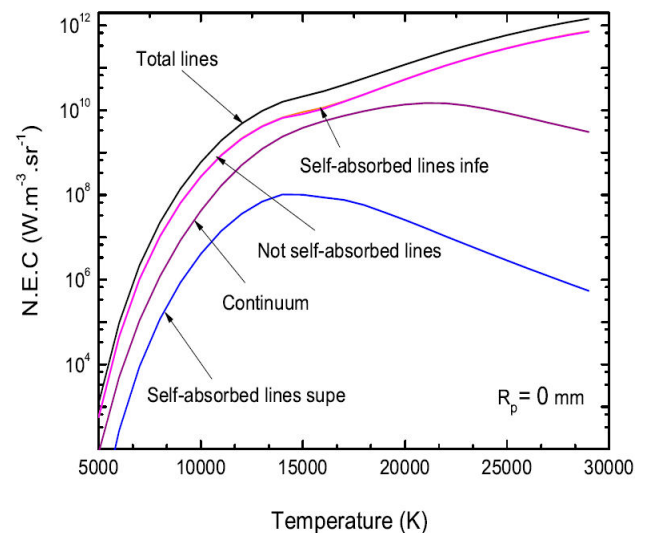


FIGURE 5. N.E.C of thin plasma composed of pure Ar at atmospheric pressure.

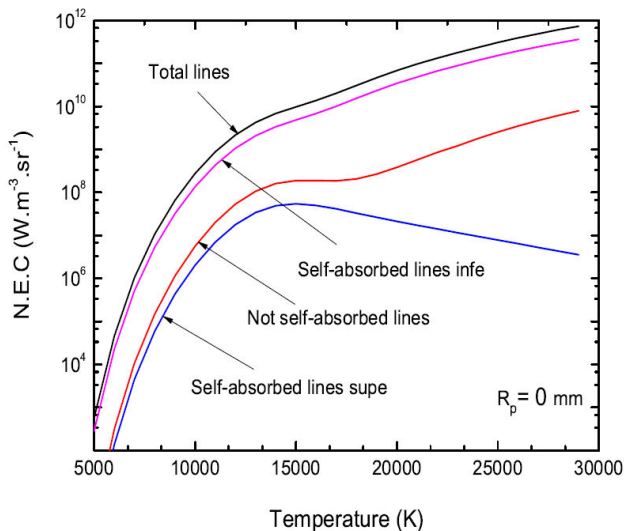


FIGURE 4. N.E.C of lines of optically thin plasma of a mixture 50% Ar–50% He at atmospheric pressure.

4.3. Contribution of lines to the N.E.C

In Fig. 4, we show the N.E.C of lines of optically thin plasma of a mixture 50% Ar–50% He at atmospheric pressure and $R_p = 0$ mm. It can be seen from Fig. 4, the total radiation emitted by the lines results from the overlay of the following contributions:

- The self-absorbed lines with a wavelength less than 200 nm.
- The self-absorbed lines with a wavelength superior than 200 nm.
- The not self-absorbed lines.

It can be seen that the self-absorbed lines whose wavelength is lower than 200 nm are the majority given the total radiation emitted by the lines.

Figure 5 shows the components of the total N.E.C of a optically thin plasma of pure Ar at atmospheric pressure and $R_p = 0$ mm. The results show that total net radiation from lines and in particular resonance lines (self-absorbed) including the wavelength is less than 200 nm and lines not self-absorbed. This figure allows to better estimate this part of radiation represented by these lines that can reach nearly $\sim 98\%$ of total radiation at low temperatures ($5000 \text{ K} \leq T \leq 14000 \text{ K}$) and high temperatures ($T \geq 20000 \text{ K}$). In these temperature intervals, the contribution of the continuum, is therefore negligible. In that region of temperatures the contribution of self-absorbed lines as well as the total lines in the total N.E.C decrease slightly but however, the majority still remains at almost $\sim 87\%$ to 14 000–20 000 K.

4.4. Influence of the proportion in N.E.C

In industrial plasma processes such as plasma spraying or gas–tungsten arc welding, He is widely used with Ar. Ar is used for its high mass density whereas He increases the enthalpy of the plasma. The presence of He also increases the thermal conductivity of the mixture compared with the pure gases and limits the penetration of the surrounding gas. Consequently, the mixture exhibits a higher viscosity due to its high ionization energy. However, He can create a departure from equilibrium because of the high excitation potential of its first excited levels and of its light mass which facilitates the diffusion phenomena.

Figure 6 shows the evolution with the temperature of the net emission coefficient total of 4 ternary plasmas Ar–He composed of: pure Ar, 80% Ar–20% He, 50% Ar–50% He and pure He. We note that as the proportion of He increases (and the proportion of Ar decreases), the values of the N.E.C

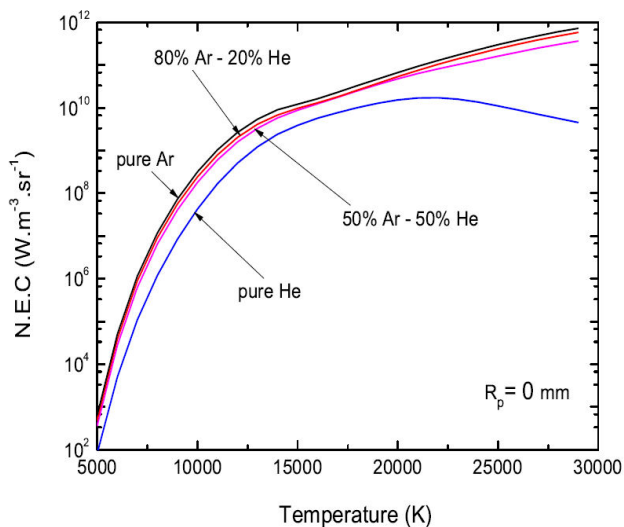


FIGURE 6. The influence of thin plasma composition Ar–He at pressure atmospheric on the N.E.C.

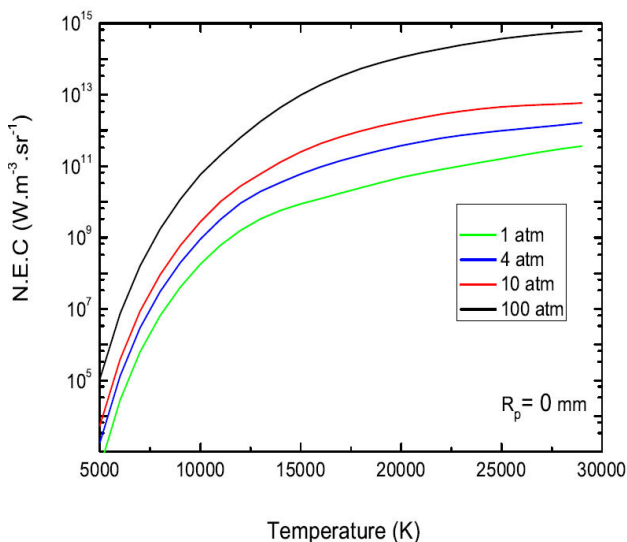


FIGURE 7. Influence of pressure N.E.C on thin plasma of a mixture 50% Ar–50% He.

decrease, ternary plasmas Ar–He. We can deduce that it is because the proportion of Ar decreases as plasma radiation intensity decreases. It is clear that the He only plays a role at very high temperatures (centre of plasma) and for important proportions. This phenomenon can be explained by a higher ionization potential for He than Ar.

4.5. Influence of pressure

We now proceed to examine the sensitivity of N.E.C to the pressure p . In Fig. 7, we show the N.E.C of a mixture 50% Ar–50% He for a radius and four values of the selected pressures $p = 1, 4, 10$ and 100 atm. This result has a double interest, show the influence of the pressure on the total N.E.C and show the linearity of this coefficient with it. We note first of all that the increase in pressure increases the net

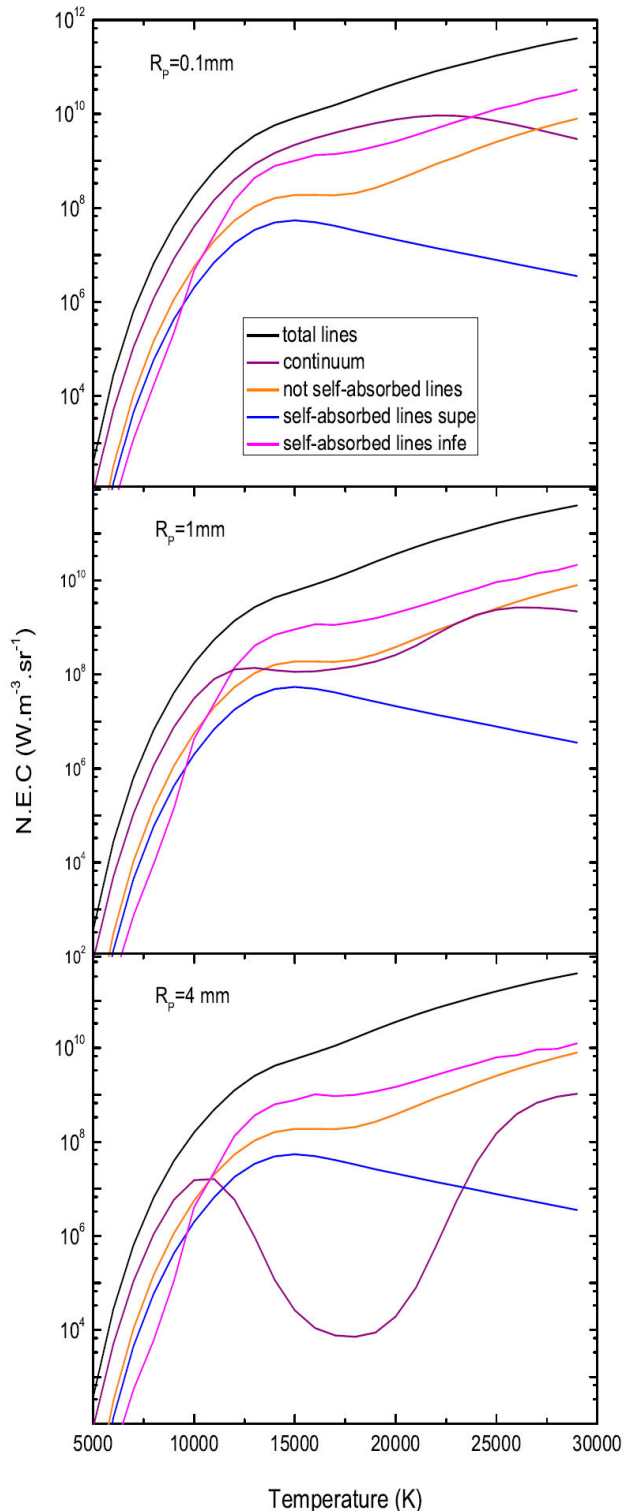


FIGURE 8. The influence of the plasma radius ($R_p=0.1, 1$ and 4 mm) upon the N.E.C from a mixture 50% Ar–50% He, at atmospheric pressure.

emission factor. The N.E.C depends only on temperature and pressure, and therefore the total density of the species. It therefore seems correct to consider the radiation proportional to the pressure. This result has a large importance to the ex-

tent that numerical models not only use also proportional to the pressure. Indeed, the profile pressure could alter the profile of a line and by these results allow us to conclude that the dependence of the N.E.C on the pressure is related not only to increase the total density of the species but also to phenomena of the widening of the lines. It can be seen from Fig. 7, these results highlight the increase in the N.E.C with pressure. Indeed, the main contribution to the N.E.C comes from line emission and the population number densities of the corresponding emitting levels are increased at high pressure. For a given temperature, the population densities of all chemical species are linked to the pressure through the perfect gas law. Thus, it is often assumed that the N.E.C is directly proportional to the pressure.

4.6. Influence of the plasma sizes

In all the results shown previously in Figs 3-7, the plasma radius R_p was taken to be constant at the value of 0 mm. We have investigated the influence of the R_p on the N.E.C.

The N.E.C depends not only on the temperature and the plasma radius but also on the pressure. Figure 8 shows the different components of the N.E.C a mixture of 50% Ar–50% He at atmospheric pressure, in an interval of temperature ranging from 5000–30 000 K and for three selected values of plasma radius (*i.e.* $R_p = 0.1, 1$ and 4 mm). It is broken down into two phases.

The first go from 5000 K to 10 000 K, the radiation of self-absorbed lines is still almost all the radiation with almost $\sim 90\%$ of the coefficient total N.E.C for the radius is equal to $R_p=0$ mm, the emission of the not self-absorbed lines, the atomic continuum is then negligible on the other hand when the radius increases in radius is equal to $R_p=0.1$ mm, $R_p=1$ mm and $R_p=4$ mm the radiation from the continuum is becoming the dominant. The second phase, including the temperatures between 10 000 K and 30 000 K, the contribution of the self-absorbed lines with a wavelongue inside 200 nm remains greater than the continuum. As a result, the self-absorbed lines are no longer the only cause of total radiation. In effect, thus the contribution of the emission of not self-absorbed lines and the atomic continuum make up nearly half of the net emission factor which will be all the more important as the thickness of the plasma will be large. These results provide a better understanding of the mechanisms involved in total radiation, their influence as a function of temperature and the thickness of the plasma, and in particular the importance of the resonance lines and their absorption.

Figure 9 represents the total N.E.C of a composite plasma 50% Ar–50% He at atmospheric pressure, for plasma thicknesses of ($R_p = 0$ mm, 0.1 mm, 1 mm and 4 mm). We find that at a fixed temperature, the total radiation of the plasma decreases as the ray of the plasma increases, thus reflecting the effect and the importance of the absorption phenomenon that increases with the optical thickness. Most of the radiation is absorbed from the very first millimetres. LHowever,

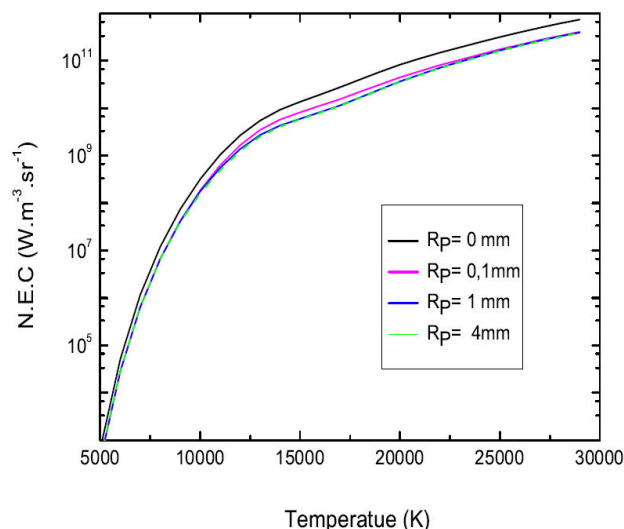


FIGURE 9. The influence of the plasma radius upon the N.E.C from a mixture 50% Ar–50% He, at atmospheric pressure.

for temperatures below ~ 12000 K, this total N.E.C varies little with the plasma radius.

5. Conclusions

The objective of this work is to calculate the radiation emitted by a thermal plasma formed by an Ar–He mixture. This radiation results from the superposition of several contributions (continuum and atomic lines). By crossing the plasma, only one fraction of the radiation manages to escape from the environment.

The first part of this paper is devoted to calculating the composition of the plasma at equilibrium which is based on the laws of thermodynamic equilibrium and from the knowledge of the functions of partition. The parameters involved in these calculations are temperature, pressure and the proportions of the mixture.

In the second part of this study, we calculated the radiative properties of established plasmas in a mixture (Ar–He) in a range of temperatures from 5000–30 000 K and for different pressure values. This study was carried out by the N.E.C method which assumes that the plasma is supposed to be homogeneous, spherical and isothermal. The results obtained show that:

- For an optically thin R_p , the N.E.C of the lines of a plasma results from the superposition of self-absorbed lines whose wavelength is less than 200 nm, self-absorbed lines with wavelength is greater than 200 nm and the not self-absorbed lines, that note self-absorbed lines with a wavelength of less than 200 nm are majority of the total radiation emitted from the lines.
- The emission coefficient of the continuum for low temperatures Ar is more emissive than He. When the tem-

perature increases the species He is the species that radiates the most.

- The increase in pressure leads to an increase in the N.E.C, it therefore seems that the radiation is proportional to the pressure.
- However, for temperatures below $\sim 12\,000$ K, this coefficient total N.E.C varies little with the plasma radius.

This result is of great importance as the numerical models not only use the net emission factor to estimate radiative losses

which lead to any modelling in plasma (calculation of thermal energy temperature profile). Analysis of the radiation emitted by a plasma also provides some information on this medium (temperature electronics, density of charged particles and degree of ionization).

Acknowledgements

Pr A K FEROUANI gratefully acknowledges the DGRSDT, Algerian Ministry of Higher Education and Research, under Project PRFU code B00L02UN130120190002.

1. P. Freton, J. J. Gonzalez and A. Gleizes, Comparison between a two- and a three-dimensional arc plasma configuration, *Journal of Physics D: Applied Physics*, **33** (2000) 2442. <https://doi.org/10.1088/0022-3727/33/19/315>.
2. M. Bouaziz, M. Razafinimanana and J. J. Gonzalez et al., An experimental and theoretical study of the influence of copper vapour on a arc plasma at atmospheric pressure, *Journal of Physics D: Applied Physics*, **31** (1998) 1570. <https://doi.org/10.1088/0022-3727/31/13/011>.
3. P. C. Huang, J. Heberlein and E. Pfender, Particle behavior in a two-fluid turbulent plasma jet, *Surface and Coatings Technology*, **73** (1995) 142. [https://doi.org/10.1016/0257-8972\(94\)02382-4](https://doi.org/10.1016/0257-8972(94)02382-4).
4. V. Aubrecht and J. J. Lowke, Calculations of radiation transfer in SF₆ plasmas using the method of partial characteristics, *Journal of Physics D: Applied Physics*, **27** (1994) 2066. <https://doi.org/10.1088/0022-3727/27/10/013>.
5. P. Fauchais, Understanding plasma spraying, *Journal of Physics D: Applied Physics*, **37** (2004) R86. <https://doi.org/10.1088/0022-3727/37/9/R02>.
6. S. Ailas, B. Liani and A. K. Ferouani, Effect of molecules in radiative emission from the thermal plasmas of CH₄-H₂ mixtures, *High Temperature Material Processes: An International Quarterly of High-Technology Plasma Processes*, **20** (2016) 279. <https://doi.org/10.1615/HighTempMatProc.2016017885>.
7. R. Hannachi, Y. Cressault and Ph. Teulet et al., Net emission of H₂O-air-MgCl₂/CaCl₂/NaCl thermal plasmas, *J. Phys. D: Appl. Phys.*, **41** (2008) 205212. <https://doi.org/10.1088/0022-3727/41/20/205212>.
8. A. Gleizes, J. J. Gonzalez and B. Liani et al., Calculation of net emission coefficient of thermal plasmas in mixtures of gas with metallic vapour, *J. Phys. D: Appl. Phys.*, **26** (1993) 1921. <https://doi.org/10.1088/0022-3727/26/11/013>.
9. J. Menart, S. Malik and L. Lin, Coupled radiative, flow and temperature-field analysis of a free-burning arc, *Journal of Physics D: Applied Physics*, **33** (2000) 257. <https://doi.org/10.1088/0022-3727/33/3/312>.
10. G. Raynal and A. Gleizes, Radiative transfer calculation in SF₆ arc plasmas using partial characteristics, *Plasma Sources Science and Technology*, **4**(1) (1995) 152. <https://doi.org/10.1088/0963-0252/4/1/017>.
11. J. J. Lowke, Predictions of arc temperature profiles using approximate emission coefficients for radiation losses, *Journal of Quantitative Spectroscopy and Radiative Transfer*, **14**(2) (1974) 111. [https://doi.org/10.1016/0022-4073\(74\)90004-1](https://doi.org/10.1016/0022-4073(74)90004-1).
12. S. Ailas, Etude du spectre moléculaire émis par un plasma thermique formé de mélange CH₄-H₂. Tesis de doctorado, University Tlemcen-Algeria, (2017).
13. H. W. Drawin and F. Emard, Optical Escape Factors for Bound and Free-bound Radiation from Plasmas. I. Constant Source Function, *Beitr. Plasma. Phys.*, **13** (1973) 143. <https://doi.org/10.1002/ctpp.19730130304>.
14. Y. Naghizadeh-Kashani, Y. Cressault and A. Gleizes, Net emission coefficient of air thermal plasmas, *J. Phys. D: Appl. Phys.*, **35** (2002) 2925. <https://doi.org/10.1088/0022-3727/35/22/306>.
15. S. Chauveau, M. Y. Perrin, Ph. Riviere et al., Contributions of diatomic molecular electronic systems to heated air radiation, *J. Quant. Spectrosc. Radiat. Transfer*, **72**(4) (2002) 503. [https://doi.org/10.1016/S0022-4073\(01\)00141-8](https://doi.org/10.1016/S0022-4073(01)00141-8).
16. Y. Cressault and A. Gleizes, Thermal plasma properties for Ar-Al, Ar-Fe and Ar-Cu mixtures used in welding plasmas processes: I. Net emission coefficients at atmospheric pressure, *J. Phys. D: Appl. Phys.*, **46** (2013) 415206. <https://doi.org/10.1088/0022-3727/46/41/415206>.
17. T. Billoux, Y. Cressault and A. Gleizes, Net emission coefficient for CO-H₂ thermal plasmas with the consideration of molecular systems, *J. Quant. Spectrosc. Radiat. Transfer*, **166** (2015) 42. <https://doi.org/10.1016/j.jqsrt.2015.07.011>.
18. B. Liani, M. Rahmouni and A. H. Belbachir et al., Computation of net emission of CH₄-H₂ thermal plasmas, *J. Phys. D: Appl. Phys.*, **30** (1997) 2964. <https://doi.org/10.1016/j.jqsrt.2015.07.011>.
19. S. Askri, A. K. Ferouani and B. Liani et al., Effect of pressure on thermodynamic properties of CH₄ thermal plasmas mixed with H₂. *High Temperature Material Processes: An International Quarterly of High-Technology Plasma Processes*, **23**(4) (2019) 365. <https://doi.org/10.1615/HighTempMatProc.2020032931>.

20. D. Godin and J. Y. Trépanier, A Robust and Efficient Method for the Computation of Equilibrium Composition in Gaseous Mixtures, *Plasma Chemistry and Plasma Processing*, **24** (2004) 447. <https://doi.org/10.1007/s11090-004-2279-8>.
21. M. W. Chase, C. A. Davies and J. R. Downey et al., JANAF thermochemical tables, *J. Phys. Chem. Ref. Data*, **14** (1985) 927.
22. G. Herzberg, *Molecular Spectra and Molecular Structure I. Spectra of Diatomic Molecules*, (Van-Nostrand-Reinhold, New York, USA, 1950).
23. K. P. Huber and G. Herzberg, *Molecular Spectra and Molecular Structure, IV. Constants of Diatomic Molecules*, (Van Nostrand Reinhold, New York, 1978).
24. J. O. Hirschfelder, C. F. Curtis and B. R. Byron, *Molecular Theory of Gases and Liquids*, (Wiley, New York, USA 1964).
25. J. Menart and S. Malik, Net emission coefficients for Argon-iron thermal plasmas, *Journal of Physics D: Applied Physics*, **35** (2002) 867. <https://doi.org/10.1088/0022-3727/35/9/306>.
26. T. Moscicki, J. Hoffman and Z. Szymanski, Net emission coefficients of low temperature thermal iron-helium plasma, *Optica Applicata*, **38** (2008) 365. <http://opticaapplicata.pwr.edu.pl/>.
27. M. Wendt, Net emission coefficients of Argon iron plasmas with electron Stark widths scaled to experiments, *Journal of Physics D: Applied Physics*, **44**(15) (2011) 125201. <https://doi.org/10.1088/0022-3727/44/12/125201>.
28. R. W. Liebermann and J. J. Lowke, Radiation emission coefficients for sulfur hexafluoride arc plasmas, *J. Quant. Spectrosc. Radiat. Transfer*, **16**(3) (1976) 253. [https://doi.org/10.1016/0022-4073\(76\)90067-4](https://doi.org/10.1016/0022-4073(76)90067-4).
29. A. Gleizes, J. J. Gonzalez and M. Razanimanana et al., Influence of radiation on temperature field calculation in SF₆ arcs, *Plasma Sources Sci. Technol.*, **1**(2)(1992) 135. <https://doi.org/10.1088/0963-0252/1/2/011>.
30. Y. Wu, C. Wang and H. Sunet et al., Properties of C4F7N–CO₂ thermal plasmas: thermodynamic properties, transport coefficients and emission coefficients, *Journal of Physics D: Applied Physics*, **51**(15) (2018) 155206. <https://doi.org/10.1088/1361-6463/aab421>.
31. M. I. Boulos, P. Fauchais and E. Pfender, *Thermal Plasmas Fundamentals and Applications*, **1** (New York, London: Plenum, USA 1994).
32. B. Liani, Calculation of the radiation emitted by arc plasmas composed of a mixture of gas and metal vapor”. Tesis de doctorado, University Paul Sabatier, Toulouse, France (1992).
33. H. W. Drawin and P. Felenbok, *Data for Plasma in Local Thermodynamic Equilibrium*, (Gauthier-Villars, Paris, France 1965).
34. NIST *Atomic Spectra Database* <http://physics.nist.gov/PhysRefData/ASD/index.html>.
35. D. Hofsaess, Emission continua of rare gas plasmas, *Journal of Quantitative Spectroscopy and Radiative Transfer*, **19**(3) (1978) 339. [https://doi.org/10.1016/0022-4073\(78\)90068-7](https://doi.org/10.1016/0022-4073(78)90068-7).
36. H. R. Griem, *Spectral Line Broadening by Plasmas*, (New York, Academic, USA 1974).
37. M. Baranger, *Atomic and Molecular Processes*, (ed D Bates, New York, Academic, USA 1962).
38. G. Traving, *Interpretation of Line Broadening and Line Shift in Plasma Diagnostics*, (ed W Lochte-Holtgreven Amsterdam, North-Holland 1968).